New Materials, Compounds and Applications
Vol.6, No.3, 2022, pp.243-251

EFFECT OF EXTENDED DEFECTS ON PHOTOLUMINESCENT PROPERTIES OF ZnTe/GaAs EPITAXIAL FILMS

Muratbay Sharibayev*, Bisenbay Kunnazarov, Marat Tagaev, Azamat Kalilaev, Gumisbek Allambergenov

Karakalpak State University, Nukus, Uzbekistan

Abstract. The radiative spectra of deep levels of ZnTe/(001) GaAs epitaxial films with different thicknesses grown by the molecular beam epitaxy method have been determined by the photoluminescence method. The change in planar stresses in ZnTe/(001) GaAs epitaxial films has been calculated from the energy shift of the photoluminescence peaks. The role of GaAs diffusion and internal stresses in epitaxial films has been discussed. It was determined that the changes in the technology of growing epitaxial ZnTe/GaAs buffer layers using molecular beam epitaxy, namely, the use of a thin recrystallized ZnTe layer (d~10 nm) and an increase in the thickness of the buffer layer lead to an improvement in the structure of the epitaxial layer (a decrease in the full width at half maximum, an increase in the size of the mosaic), as well as an increase in the overall intensity of the photoluminescent bands in the exciton region of the specter. As the result of the study, the influence of extended defects in the near-surface region of the ZnTe/GaAs epitaxial layer on the deviation from the stoichiometric composition during the growth of the ZnTe film was determined, which leads to saturation of the surface with Te atoms that fall into precipitates with the formation of dislocation. The study of the optical characteristics of ZnTe/GaAs epitaxial films made it possible to determine the composition of the films, the contamination of the film, and the change in the composition of the films during growth.

Keywords: *photoluminescence, epitaxial films, deformation, intensity, film thickness, mechanical stress, quantum well.*

Corresponding Author: *Muratbay Sharibayev, Department of Physics, Karakalpak State University, Nukus, Uzbekistan, e-mail: msharibayev@inbox.ru*

Received: *6 July 2022;* ***Accepted:*** *17 November 2022;* ***Published:*** *7 December 2022*

1. Introduction

The interest in the radiation of quantum-dimensional structures based on A_2B_6 materials is due to the possibility of manufacturing injection sources of coherent (Brandão & Cavalcanti, 2019) and incoherent radiation, as well as emitters with electron pumping (Cuesta *et al.*, 2022), covering almost the entire visible range, based on these structures. The method of low-temperature photoreflectance, photoluminescence (PL) (the temperature of low-temperature photoluminescence (LT PL T) = 4.2 and 77 K) was used to study the EL qualities and the ZnTe and ZnTe/GaAs interface boundaries. It is known that when ELs, A_2B_6 semiconductors are grown, a transition layer with a high density of dislocations and other extended defects is formed on GaAs substrates near the interface (Luo *et al.*, 2020), which affect the optical properties of EL and stimulate degradation processes of light-emitting devices manufactured on their basis (Cao *et al.*,

How to cite (APA):
Sharibayev, M., Kunnazarov, B., Tagaev, M., Kalilaev, A., Allambergenov G. (2022). Effect of extended defects on photoluminescent properties of ZnTe/GaAs epitaxial films. *New Materials, Compounds and Applications*, *6*(3), 243-251.

2021; Pal & Pal 2021; Xie *et al.*, 2022). This makes the issue of identifying bands associated with extended defects (including dislocations) in the EL A_2B_6 more relevant.

In the PL and cathodoluminescence spectra of ZnTe EL and single crystals obtained with different methods, an intense I_1^C radiation band ($h\nu$ =2.357 eV at 4.2 K) is often found. It is believed to be caused by the radiative recombination of excitons bound to either an isolated neutral acceptor (Si_{Te}) or an acceptor (V_{Zn}) located near mismatch dislocations (vacancy-dislocation complex) (Yang *et al*., 2020). Thus, the nature of this band has not yet been definitively established.

In order to determine the nature of the luminescent centers responsible for the I_1^C band, the influence of the following parameters on the PL spectra of ZnTe buffer EL: (I) the thin (~5-10 nm) intermediate recrystallized ZnTe layer, located between the buffer layer and the substrate (100) GaAs; (ii) the thickness of the buffer layer, and (III) the buildup of the quantum-dimensional layers of $Cd_xZn_{1-x}Te/ZnTe$ (x=0.2-0.4) will be investigated. In addition, the spatial distribution (by buffer depth) of the intensity (I) and spectral position (λ_m) of the I_1^C band, as well as the temperature dependences of I and λ_m, were explored. At the same time, X-ray diffraction measurements of the swing curves were carried out to control the structural perfection of the ZnTe EL.

2. Methods

All structures with different thicknesses were obtained by molecular beam epitaxy (MBE) at the KATUN facility. Simulatenously, high purity elements were deposited on semi-insulating substrates (GaAs). The GaAs surface cleaning was performed by heating in a vacuum at a temperature of ~550-580^{0}C. The growth process was controlled by the method of reflection high-energy electron diffraction (RHEED). The cultivation of ZnTe layers was carried out in two ways. The first method (Process 1) is as follows. After cooling of the substrate to 250-280^{0}C, Zn and Te molecular beams were applied to it, the ratio of which was equal to the ratio of the Zn and Te equivalent pressures. This led to the reconstruction of the a(2x1) surface and its stabilization by tellurium. After growing the film at 10 nm, the temperature was increased to 350 ^{0}C. The epitaxy was performed at the same temperature and with the above-mentioned ratios of Zn/Te molecular beams, which ensured the simultaneous existence of the reconstruction of surfaces a(2x1) and c(2x2), providing growth conditions close to stoichiometry. In the other method, to improve the growth conditions, an amorphous ZnTe layer was applied to the substrate, which then crystallized in the tellurium flow at t =400-450 ^{0}C. After crystallization, the system was cooled to 250-280^{0}C, and afterward, technological operations were carried out as in the first method.

Measurements of the PL spectra in the range from 1.4 eV to 2.4 eV were carried out in the temperature range from 4.2 to 80 K on an automated system with a grating monochromator, and in the range of 0.6-1.4 eV with a prism monochromator. The PL spectra were excited by argon laser radiation with λ_1=0.51453 microns and λ_2=0.488 microns. PL spectra were measured on a three-prismatic glass spectrograph ISP-51 and the basis of a grating spectrometer MDR-23. The initial parameters and some technological conditions for obtaining the studied EL and structures are given in Table 1.

Table 1. Initial Parameters for ZnTe Film

Samples No	EL, λ_m	ZnTe layer, 5 nm	QW	ZnTe, amorphous layer 40 nm	The full width at half maximum (FWHM), arc s
147	5.7	+	-	-	~ 90
144	3	+	-	-	~127
67	2.7	+	-	-	~ 312
90	1.5	+	-	-	~ 360
88	1.5	-	-	-	~ 560
114	1.5	+	3 QW $Cd_{0.3}Zn_{0.7}Te$ $L_1=L_2=L_3=2$ nm, $L_B=30$ nm	+	-

3. Results and discussion

Fig.1 shows a typical PL spectrum of the ZnTe/GaAs buffer EL at 4.2 K in the wavelength range of 510-630 nm. As can be seen from the figure, in the short-wavelength region of the spectrum one can see emission lines of a free exciton (I_{FX}) split by biaxial tensile stresses into two components: I_{FX}^{hh} (X_{IS}; m_j=+3/2) and I_{FX}^{lh} (X_{IS}; m_j=+1/2). In this case, the I_{FX}^{hh} component corresponds to the line with hν=2.379 eV, and the I_{FX}^{lh} component corresponds to the hν=2.374 eV line, which is a superposition of I_{FX}^{lh} and the exciton emission line bound to a neutral donor (I_2^{Ga}) (Yang *et al.*, 2020).

In addition to those describedone can also see an intense I_1^C band with $h\nu_m$ = 2.356 eV in the exciton region of the spectrum and a band with $h\nu_m$ =2.352 eV (I_2^C) of lower intensity near it on the long-wavelength side (Fig. 1). In samples with quantum layers on the short-wavelength side of I_1^C, an additional I_X band with $h\nu_m$ =2.359 eV is observed (Fig. 2 a, b, respectively). The I_1^C band is not elementary, since in some samples it is possible to observe a distinct shoulder at the long-wavelength edge of the band. The bands located near I_1^C are accompanied by phonon repetitions with the electron-phonon coupling factor s≈0.2 (Fig.1). In the longer wavelength region of the spectrum, much less intense (compared to I_1^C) bands Y_1 ($h\nu_{m1}$=2.189 eV, 4.2 K) and Y_2 ($h\nu_{m2}$=2.147 eV, 4.2 K) were observed. The use of an intermediate ZnTe layer (Process II), as well as an increase in the thickness of the EL, leads to an increase in the intensity of all bands in the exciton region and a decrease in the intensity of the impurity band λ=650 nm, as well as to a decrease in the intensity of the bands Y_1 and Y_2. With the thickness of the layers ~2.7 microns, these bands are practically absent. It should be noted that the ratio of band intensities I_2^{Ga}/I_{FX}^{hh}; I_1'/I_{FX}^{hh} practically does not change during the transition from a sample with a thickness of 1.5 microns to a sample with a thickness of 2.7 microns (λ_{exc} =0.488 microns), and I_1^C/I_{FX}^{hh} increases slightly.

In addition to the change in intensity of the bands, the position of their maxima also shifted (Table 1). The position of the maximum of the bands of free I_{FX}^{hh}, as well as the bound excitons I_2^{Ga} (I_{FX}^{lh}), I_1', and the I_1^C band in all layers, is shifted towards lower energies compared to their position in the bulk material (E=2.3805±0.0003 eV, 4.2 K), which is due to the presence of planar tensile stresses ∑. At the same time, the displacement value is maximal in samples obtained without an intermediate layer, and in samples with an intermediate layer, it decreases with increasingin EL thickness, which indicates a decrease in stresses. The superlattice deposition leads to a noticeable shift of the band maxima towards lower energies, i.e., an increase in tensile stresses.

The values of the levels of residual deformations are given in Table 1. Their calculation was performed using the strain potential constants potential according to the formulas given in Mohanty (2018). Significantly, the spectral position of the I_2^{Ga} and I_1' bands shift approximately the same with increasing voltages, and I_1^C is weaker, which is consistent with the data Bonef et al. *(*2018).

Since in the work Khan et al. (2022) identifying I_1^C as an exciton bound to a zinc vacancy near the dislocation, it was assumed that this radiation occurred mainly in the region of the GaAs-ZnTe interface, we investigated the intensity distribution I_1^C over the depth of the epitaxial layer using layer-by-layer stripping of samples with a step of ~0.1 microns.

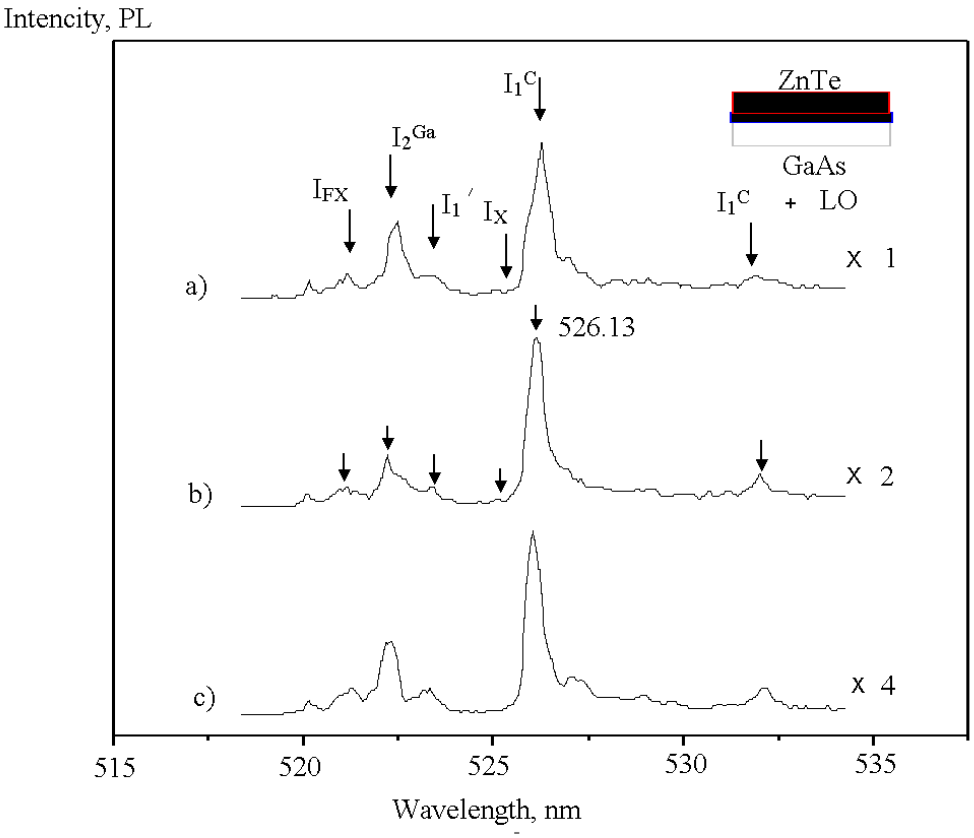

Fig. 1. PL spectra of ZnTe/GaAs EL with a thickness of 1.5 microns and 2.7 microns (curve a,b) grown with the use of process I and process II (curve c)

Fig. 2 shows the temperature dependences of the intensity and positions of the maxima ($\Delta E_{max} = h\nu_{4.2} - h_T$) of the bands in the exciton region of the spectrum of ZnTe/GaAs EL with the thickness of 1.5 microns and a quantum well (QW) (No. 5). AS the temperature rises above 15 K, all these bands begins to decrease in intensity.

In this case, the intensity of the I_2^{Ga} band varies similarly to the intensity of the I_{FX}^{hh} band. At the same time, the slope of the temperature dependence of the I_1^C band is significantly steeper in this temperature range (>15 K) and corresponds to the activation energy $> \Delta E_a \sim 0.008\ eV$. Along with the decrease in the intensity of the PL bands with an increase in temperature, the spectral position of the emission lines of free (I_{FX}^{hh}) and

bound (I_2^{Ga} and I_1') excitonswith a thermal shift coefficient $dE/dT \sim 0.16 meV/K$ in the temperature range of 20−80 K is shifted to the low-wavelength side.

Temperature dependence of the PL spectra

At the same time, the position of the I_1^C and I_X lines practically does not change up to a temperature of 80 K. As can be seen from the above results, several characteristics of the bands in the I_1^C group differ from the corresponding characteristics of both free and bound excitons. This difference is manifested in the absence of a shift in the position of the maxima of these bands, λ_{max}, with a temperature change from 4.2 to 80 K, as well as in a weaker shift of λ_{max} than that of I_{FX}^{hh} and I_2^{Ga} with a change in the magnitude of deformations. The latter is evidenced by the dependence of the positions of I_1^C and exciton lines on the presence or absence of an intermediate layer and the thickness of the EL, as well as the displacement of I_1^C and Iõ during layer-by-layer stripping of the latter. Note that a weak shift in I_1^C position with increasing of the EL thickness was also observed in Gonnissen et al. (2017) and was explained by thecorresponding band radiative centers were located mainly in the deeper layers adjacent to the interface between the ZnTe/GaAs, where the mechanical compressive stress near the heterointerface partially offset planar tensile stress in more near-surface layers., In particular, this allowed the authors of Salazar-Tovar et al. (2020) to associate the centers responsible for the I_1^C band with defects near mismatch dislocations.

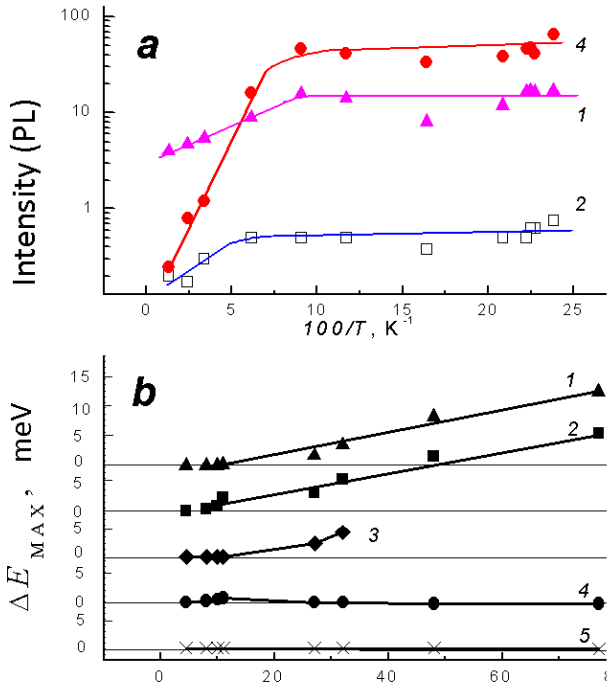

Fig. 2. Temperature dependence of the intensity (a) and the spectrum of the half-width maximum (b) in the range of 4.2÷80K of the ZnTe/GaAs EL with a single QW

However, as experiments on layer-by-layer EL stripping show, the intensity of the I_1^C band decreases deep into the layer. It is significant that with increasing EL thickness, the magnitude of elastic deformations decreases, and the intensity of the I_1^C band

increases. Such anticorrelation of I_1^C and ε may indicate in favor of its connection with extended defects, but not with misfit dislocations, since I_1^C/I_{FX} and I_X/I_{FX} decrease after stripping.

It is known that in the PL and cathodoluminescence spectra of undoped ZnTe EL obtained by various methods (molecular beam epitaxy (MBE), metalorganic vapour-phase epitaxy (MOVPE)) and ZnTe single crystals often show an intense radiation band I_1^C (hν=2.357 eV at 4.2 K). Their nature has not yet been established. Among its features, one can note a sharp decrease in intensity with an increase in the concentration of residual impurities and during doping, a strong dependence of intensity on growth conditions, and a weak one on temperature. This band is believed to be caused by the radiative recombination of excitons bound at deep neutral acceptors. Either a neutral two-charge acceptor Si_{Te} or V_{Zn} located near the mismatch dislocations are considered as such acceptors. The intensity of this band decreased with the increase in layer thickness (up to 11 microns) and we have concluded that this band is associated with an area near the interface in which mismatch dislocations are located, the formation of which may be accompanied by the appearance of V_{Zn}. At the same time, it should be noted that the presence of structural defects (mainly mismatch dislocations) in most works dealing with the study of ZnTe/GaAs EL (see, for example, Teisseyre et al. (2021)) is usually associated with deeper Y-bands, which is confirmed by a decrease in their intensity with a decrease in mismatch stresses as a result of replacing the GaAs substrate with GaSb and ZnTe. Fig. 3 shows a weak change in the PL band of ZnTe/GaAs epitaxial films. With a further increase in temperature (T > 15 K), their noticeable quenching occurs. In this case, the intensity of the I_2^{Ga} band decreases as does the decrease in intensity of the I FX band. At the same time, the slope of the temperature dependence $\ln I_1^C = f(1/T)$ in this temperature range is noticeably sharper and corresponds to the activation energy ΔE_a = 0.008 eV. In addition to the decrease in the intensity of the PL band with increasing temperature, there is a shift of the spectral position of emission lines of free excitons (I_{FX}) and excitons bound to a neutral donor (I2Ga) and a neutral acceptor ($I_1^{|}$) in the long-wavelength side with the coefficient of thermal shift ($^{dE}/_{dT} \sim 0.15 meV/K$) almost the same for the I_{FX} and I_2^{Ga} bands in the temperature range of 20-80 K. Note that the displacement is weaker than the temperature variation of the bandgap width of ZnTe single crystals given in the literature ($^{dE}/_{dT} \sim 0.36 meV/K$). This may be due to a change in the level of residual deformations in the ZnTe/GaAs EL when the sample is heated from 4.2 to a temperature of 80K. It is significant that the position of the I_1^C and I_X lines practically does not change up to a temperature of 80 K. Regarding single A_2B_6 crystals, it is known that when they are grown, saturation occurs for one of the components, so for CdS and CdSe (Sharibaev, 2019), there is always saturation for Cd during the growth process. It is also known that the p-type of conductivity of ZnTe single crystals is determined by excess Te. In such crystals of the near-surface region, near-surface layers enriched with Te have been repeatedly observed.

Since the intensity of the I_1^C band increases with the size of the mosaic, it can be assumed that the centers that determine the nature of the I_1^C series are associated with defects inside the disoriented blocks, possibly with the boundaries of the sub-blocks that make up the mosaic and have a dislocation origin. They create acceptor-type levels in the forbidden zone. In this case, the I_1^C transition may be associated with the radiative recombination of excitons bound at dislocations.

When using an intermediate recrystallized layer, the intensity of the Y_1 and Y_2 lines decreases, and at a thickness of ~2.7 microns, these bands are practically absent. It should be noted that the ratio of the intensities of the bands $I_2^{Ga}/I_{FX}^{hh}I_1^1/I_{FX}^{hh}$ during the transition from the sample with a thickness of 1.5 μm for the sample with a thickness of 2.7 μm is almost constant (λ_{exc}=0.488 μm), and the ratio of the bands I_1^C/I_{FX}^{hh} grows a little. Since the Y_1 и Y_2 bands are associated with exciton recombination on mismatch dislocations, a decrease in their intensities with an increase in thickness<1 μm from the region near the ZnTe/GaAs interface only proves the correctness of the assumption made since misfit dislocations are localized in this region. Reduction of the intensities of the Y_1 и Y_2 bands when using a thin intermediate layer with an unchanged ratio of the lines of bound excitons $I_{FX}(I_2^{Ga}/I_{FX}^{lh}$; $I_1^1/I_{FX}^{hh;}$; $^{I}{}_1^C/I_{FX}^{hh})$ may be a consequence of a decrease in the concentration of dislocations due to changes in planar stresses in the EL.

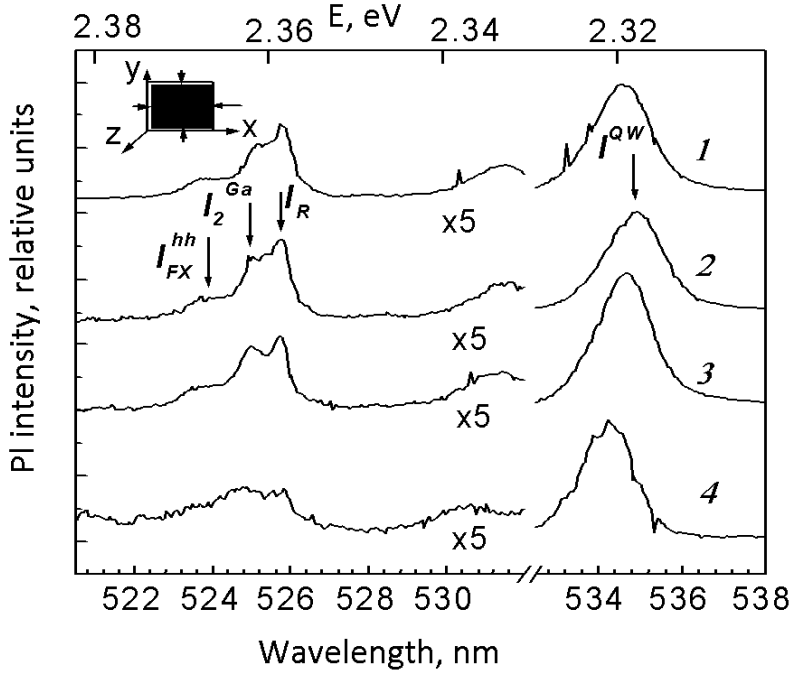

Fig. 3. Temperature dependence of intensity in the range of 4.2-80 K of ZnTe/GaAs EL with one QW

Indeed, the position of the maximum of the bands of free I_{FX}^{hh}, as well as the bound excitons $I_2^{Ga}(I_{FX})$, $I_1^{'}$, and the I_1^C band in all layers, is shifted towards lower energies compared to their positions in the bulk material E=2.3805±0.0003 eV, 4.2 K (Zhang *et al.*, 2013), which is probably due to the presence of planar tensile stresses. Knowing the relative values of the displacement ΔE_{lh} and ΔE_{hh} are known for free exciton lines with light holes I_{FX}^{lh} and heavy holes I_{FX}^{hh}, it is possible to approximately estimate the magnitude of the planar stresses ε for ZnTe/GaAs EL of different thickness. It is known that:

$$\Delta E_{hh} = \left(-2a\frac{C_{11}-C_{12}}{C_{11}} + b\frac{C_{11}+2C_{12}}{C_{11}}\right)\cdot\varepsilon \qquad (1)$$

$$\Delta E_{lh} = \left(-2a\frac{C_{11}-C_{12}}{C_{11}} - b\frac{C_{11}+2C_{12}}{C_{11}}\right)\cdot\varepsilon \quad (2)$$

where C_{ij} is the elastic stiffness coefficient, a is the hydrostatic displacement potential, and b is the deformation displacement potential.

Using the literature data Zhang, (2013); Nakasu et al. (2017); Zhang et al. (2013): C_{11}=7.19*10^6 N*cm^{-2} C_{12}=4.07*10^6 N*cm^{-2}: a=-5.4 eV b=-1.8 eV, we obtained ΔE_{hh}=0.78·ε eV: ΔE_{lh}=849·ε eV. Then: ε=*ΔE= $\Delta E(X_{lh}-X_{hh})/(\Delta E_{lh}-\Delta E_{hh})$ =0.13*10^{-3} (MeV).

It appears that the displacement value is maximum for samples with an intermediate layer, and it decreases with increasing EL thickness indicating a decrease in the corresponding stresses.

The application of the CdZnTe sublattice leads to an additional shift of the band maxima lower energies, which corresponds to an increase in tension.

3. Conclusion

The main obstacle to the industrial use of ZnTe/GaAs single crystals is their low degradation resistance. Single crystals are used as a substrate. However, the use of GaAs as a substrate leads to several new problems. First, the existence of inconsistencies in constant lattices between binary ZnTe and GaAs binary compounds. For example, for a ZnTe/GaAs pair, it is ~7.6% at room temperature, and the difference in the coefficients of thermal expansion between them leads to the appearance of elastic stresses. One of the ways to influence the characteristics of the boundary of the interface between A^2B^6/GaAs structures is the use of thin intermediate layers that can delay the processes of interdiffusion of film and substrate components. For this reason, we have investigated the distribution of structural defects (typical and extended) over the depth of specially undoped ZnTe. It is shown that the changes in the technology of MBE cultivation of buffer ZnTe/GaAs ELs, such as (1) the use of a thin recrystallized layer of ZnTe (d~10 nm), and (2) increasing the thickness of the buffer layer leads to improvement of the structure of EL (decrease in FWHM, increase the size of the mosaic), as well as increase the overall intensity of the PL bands in the exciton region of the spectrum and decrease of their intensity in the impurity region (reduction in the concentration of deep centers of recombination). The paper also provides additional information about the nature of the I_1^C band and the I_X band found near it. The difference in the temperature and deformation dependences of the positions of these bands from the corresponding characteristics of the exciton emission lines, as well as an increase in their intensity with a decrease in deformations, made it possible to associate these bands with extended defects. This conclusion is confirmed by the similarity of their behavior with the behavior of the dislocation radiation (DR) bands in single A_2B_6 crystals. Based on these data, and the results of X-ray diffraction measurements, it is assumed that the centers responsible for the I_1^C band are associated with the subunit boundaries in the mosaic structure. Thus, the structural defects in the near-surface region of the ZnTe/GaAs EC possibly appear due to a deviation from the stoichiometric composition during the growth of the ZnTe film, resulting in saturation of the surface with Te atoms that fall into precipitates with the formation of dislocation.

References

Bonef, B., Grenier, A., Gerard, L., Jouneau, P.-H., André, R., Blavette, D., & Bougerol, C. (2018). High spatial resolution correlated investigation of Zn segregation to stacking faults in ZnTe/CdSe nanostructures. *Applied Physics Letters*, *112*(9), 093102. https://doi.org/10.1063/1.5020440

Brandão, P.A., Cavalcanti, S.B. (2019). Scattering of partially coherent radiation by non-Hermitian localized structures having parity-time symmetry. *Phys. Rev. A*, 100, 043822. https://doi.org/10.1103/PhysRevA.100.043822

Cao, L., Klimes, K., Ji, Y., Fleetham, T. & Li, J. (2021). Efficient and stable organic light-emitting devices employing phosphorescent molecular aggregates. *Nat. Photonics*, 15, 230–237. https://doi.org/10.1038/s41566-020-00734-2

Cuesta, S., Harikumar, A. & Monroy E. (2022) Electron beam pumped light emitting devices. *Journal of Physics D: Applied Physics 55*(27), 273003. https://doi.org/10.1088/1361-6463/ac6237

Gonnissen, J., De Backer, A., den Dekker, A.J., Sijbers, J., & Van Aert, S. (2017). Atom-counting in High Resolution Electron Microscopy:TEM or STEM – That's the question. *Ultramicroscopy*, 174, 112-120. https://doi.org/10.1016/j.ultramic.2016.10.011

Khan, A.R., Zhang, L., Ishfaq, K., Ikram, A., Yildrim, T., Liu, B., ... & Lu, Y. (2022). Optical Harmonic Generation in 2D Materials. *Advanced Functional Materials*, *32*(3), 2105259.

Luo, X., Meng, W.-W., Chen, G.-X.-J., Guan, X.-X., Jia, S.-F., Zheng, H. & Wang, J.-B. (2020). First-principles study of stability, electronic and optical properties of two-dimensional Nb2SiTe4-based materials. *Acta Phys. Sin.*, *69*(19), 197102. https://doi.org/10.7498/aps.69.20200848

Mohanty, D., Sun, X., Lu, Z., Washington, M., Wang, G.-C., Lu, T.-M., Bhat, I.B. (2018). Analyses of orientational superlattice domains in epitaxial ZnTe thin films grown on graphene and mica. *Journal of Applied Physics*, *124*(17), 175301. https://doi.org/10.1063/1.5052644

Nakasu, T., Sun, W., Kobayashi M. & Asahi T. (2017). Effect of Zn and Te beam intensity upon the film quality of ZnTe layers on severely lattice mismatched sapphire substrates by molecular beam epitaxy. *Journal of Crystal Growth*, 468, 635-637. https://doi.org/10.1016/j.jcrysgro.2016.11.035

Pal, N., Pal, B.N. (2021). Chapter 19 - Solution-processed light-emitting devices. In: Das S. and Dhara S. (eds.) *Chemical Solution Synthesis for Materials Design and Thin Film Device Applications*, 623-647. Elsevier. https://doi.org/10.1016/B978-0-12-819718-9.00023-6.

Salazar-Tovar, M.U., Sutara, F. & Hernández-Calderón, I. (2020). Observation of a non-constant Cd diffusion coefficient during the thermal annealing of Zn1-xCdxSe quantum wells. *Journal of Alloys and Compounds*, 846,155698.

Sharibaev, M. (2019). Determination by photoluminescence of extended defects in epitaxial ZnTe/GaAs films. *Semiconductor Physics and Microelectronics*, 4, 45-48.

Teisseyre, H., Jarosz, D., Marona, L., Bojarska, A., Ivanov, V., Perlin, P., & Czyszanowski, T. (2021). Homoepitaxial ZnO/ZnMgO Laser Structures and Their Properties. *Phys. Status Solidi A*, *218*(1), 2000344. https://doi.org/10.1002/pssa.202000344

Xie, Y., Liu, W., Deng, W., Wu H., Wang W., Si Y., Zhan X., Gao C., Chen X.-K., Wu H., Peng J. & Cao Y. (2022). Bright short-wavelength infrared organic light-emitting devices. *Nat. Photon*., 16, 752–761. https://doi.org/10.1038/s41566-022-01069-w

Yang, H., Jing Ru Zh., Wentao C., Jin Zh., & Ji H.W. (2020). Screw-Dislocation-Driven Hierarchical Superstructures of Ag-Ag2O-AgO Nanoparticles. *Crystals*, *10*(12), 1084.

Zhang, L., Ji Z., Huang, S., Wang, H., Xiao, H., Zheng, Y., Xu, X., Lu Y., & Guo, Q. (2013). Effect of substrate temperature on optical properties and strain distribution of ZnTe epilayer on (100) GaAs substrates. *Thin Solid Films*, 536, 240-243. https://doi.org/10.1016/j.tsf.2013.04.040